

# Formation of Ionization-Cone Structures in Active Galactic Nuclei: I. Stationary Model and Linear Stability Analysis

V. L. Afanasiev<sup>1</sup>, S. N. Dodonov<sup>1</sup>, S. S. Khrapov<sup>2</sup>, V. V. Mustsevoi<sup>2</sup>, A. V. Moiseev<sup>1</sup>

<sup>1</sup> Special Astrophysical Observatory, RAS, Nizhnii Arkhyz, Karachai-Cherkessian Republic, 357147 Russia

<sup>2</sup> Volgograd State University, Volgograd, 400062 Russia

received: September 21, 2006/ revised: November 24, 2006

**Abstract.** We discuss causes of the formation of the observed kinematics and morphology of cones of ionized matter in the neighborhood of the nuclei of Seyfert galaxies. The results of linear stability analysis of an optically thin conic jet where radiation cooling and gravity play an important part are reported. The allowance for radiation cooling is shown to result in strong damping of all acoustic modes and to have insignificant effect on unstable surface Kelvin–Helmholtz modes. In the case of waveguide–resonance internal gravity modes radiative cooling suppresses completely the instability of waves propagating away from the ejection source and, vice versa, reduces substantially the growth time scale of unstable sourceward propagating modes. The results obtained can be used to study ionization cones in Seyfert galaxies with radio jets. In particular, our analysis shows that surface Kelvin–Helmholtz modes and volume harmonics are capable of producing regular features observed in optical emission-line images of such galaxies.

## 1. Introduction

Observations of many Seyfert galaxies in emission lines ( $H_\alpha$ , [OIII], etc.) suggest that Narrow Line Regions (NLRs) in these galaxies often have conic shapes. The [OIII]/ $H_\alpha$  line intensity ratio maps constructed by some authors (see, e.g., Pogge, 1989; Falcke et al., 1998) also suggest that gas in NLRs is located inside cone-shaped (sometimes bipolar) structures with opening angles  $30^\circ - 110^\circ$  and linear sizes ranging from several tens of parsecs to 20 kpc (see Table 3 in the paper of Wilson & Tsvetanov, 1994).

A number of authors thoroughly analyzed the structure of NLR in individual galaxies, such as Mrk 3 (Pogge & De Robertis, 1993; Capetti et al., 1998), Mrk 573 (Tsvetanov & Walsh, 1992; Ferruit et al., 1999), NGC 3516 (Miyaji et al., 1992; Veilleux et al., 1993), NGC 5252 (Wilson & Tsvetanov, 1994; Moorse et al., 1998), and ESO 428-G14 (Falcke et al., 1996). The above authors point out good correlation between the directions of ionized cones and those of radio jets — their symmetry axes coincide to within  $5 - 10^\circ$  (Wilson & Tsvetanov, 1994; Falcke et al., 1996; Nagar et al., 1999). Figure 1 shows, as an example, two [OIII] emission-line images of ionization cones in the galaxies NGC 3516 (Sy 1 type) and NGC 5252 (Sy 1.9 type) and the orientation of the axes of their radio jets.

The orientation of the cones with respect to galaxy disks differs from one galaxy to another, however, Wilson & Tsvetanov (1994) point out that in late-type galaxies the cone symmetry axes are virtually perpendicular to the disk plane, whereas in early-type galaxies they are inclined at small angles to the disk.

The profile of narrow emission lines in the central regions of the cone has a complex multicomponent structure. This is indicative of several systems of gaseous clouds being observed at the corresponding locations along the line of sight with mutual velocities as high as several hundred  $\text{km s}^{-1}$  (Capetti et al., 1998; Kaiser et al., 2000; Emsellem et al., 2006). In a number of cases, emission-line images of the galaxies considered exhibit a Z(S)-shaped pattern (Fig. 1) or other regular structures. High spatial resolution HST images of Seyfert galaxies (Capetti et al., 1996; Falcke et al., 1998) indicate that the Z-shaped pattern begins in the circumnuclear region (at galactocentric distances of 10–100 pc) and extends out to much larger galactocentric distances (several kpc). The NGC 3516 galaxy (Fig. 1a and Miyaji et al., 1992) shows Z-shaped filaments in the region  $r < 10 - 14''$  ( $\sim 2$  kpc) with the Northeastern part of the cone extending out to more than 6 kpc. The NLR in the NGC 5252 galaxy (Fig. 1b and Morse et al., 1998) also has a symmetric Z-like shape in the central region  $r < 10 - 15''$  (5–7 kpc), whereas the biconical structure itself, which contains regular emission-line “arcs” can be observed out to 18 kpc from the center.

Send offprint requests to: A.V. Moiseev, e-mail: moisav@sao.ru

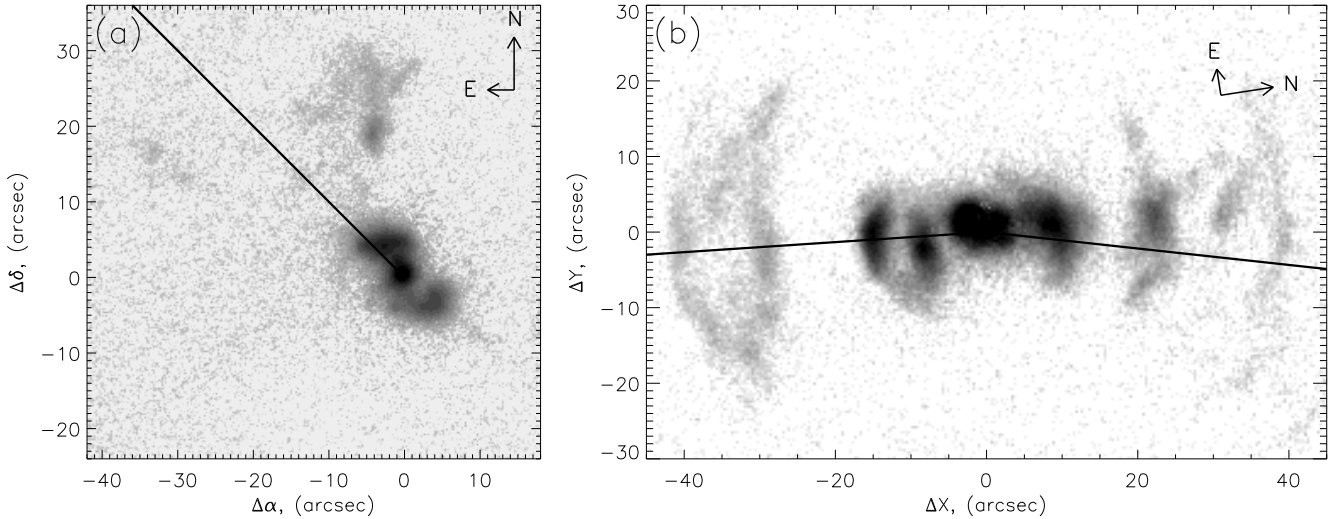


**Fig. 1.** The [OIII]-line images of ionization cones with Z-shaped patterns obtained from observations carried out at the 6-m telescope of the Special Astrophysical Observatory of the Russian Academy of Sciences (Moiseev et al., 2000). The line indicates the orientation of radio jet according to Miyaji et al. (1992) and Wilson & Tsvetanov (1994). (a) NGC 3516, (b) NGC 5252.

The motions of ionized gas inside cones are complex and poorly studied. Two-dimensional velocity fields have been constructed in a few cases (Veilleux et al., 1993; Ferruit et al., 1999; Moiseev et al., 2000), which show that different portions of Z-shaped patterns can be both “blue-” and “redshifted” with respect to the nucleus. Moreover, in some galaxies, like, e.g., in NGC 5252, the velocity fields in the region of “arcs” at large distances from the nucleus exhibit emission-line filaments that are blueshifted exclusively in one cone and redshifted exclusively in the diametrically opposite cone.

Ionization cones are believed to be due to the collimation of ionizing radiation by the torus of matter accreting onto a supermassive black hole at the nucleus of the galaxy. However, such a scenario of cone formation fails to explain the presence of regular structures. Wilson (1993) argues that ionized matter moves away from the galactic center, i.e., that it constitutes a weakly collimated jet. Capetti et al. (1996) carried out a detailed spectrophotometric study of such a Z-shaped emission-line region in the Mrk 573 galaxy and pointed out that radiation of the nucleus is evidently insufficient to produce the observed NLR and that an additional local ionization source is required. Ferruit et al. (1999), who used panoramic spectroscopy to analyze this object, also concluded that in Mrk 573 the necessary additional contribution to ionization is provided by shocks produced by the intrusion of the jet from the active nucleus into the surrounding clouds of interstellar gas.

There is no consensus of opinion as to what causes the formation of regular structures observed in ionization cones. The model of the interaction of the jet with gaseous clouds in the circumnuclear region developed by Rossi et al. (2000) explains a number of morphological fea-

tures, but fails to describe the development of symmetric Z-shaped features.

A number of researchers (see, e.g., Veilleux et al., 1993; Steffen, 1997) believe such features to be helical shocks, which are due to the presence of a highly collimated thin precessing jet. However, the hypothesis that this is the case for all the objects discussed here appears to be too daring to say at least. Mulchaey et al. (1992) interpreted the Z-shaped structure in NGC 3516 in terms of the bipolar outflow model where ejected gas is deflected toward the galactic disk. Morse et al. (1998) explain the kinematic structure observed in NGC 5252 by the presence of three ionized gas disks rotating in differently tilted planes. In addition to the above scenarios there is the possibility that excitation of a helical shock may be due to shear instability, which develops at the layer between the matter of collimated radio jet and ionized gas moving at different velocities (Falcke et al., 1996).

We begin a series of papers where we naturally show with no additional assumptions that the observed structures and velocity fields can be explained in terms of the following scenario, which agrees with the unified model of the activity of galactic nuclei (Antonucci, 1993; Wills, 1999):

- the highly collimated high-velocity bipolar jet (radio jet) breaks through the torus of optically opaque matter accreting onto the supermassive central object (black hole) in two diametrically opposite directions parallel to the proper angular momentum of the torus matter;
- the jet matter squeezed by the ambient pressure heats up intensively and expands rapidly toward the initial ejection through the narrow channel thus produced;

- the internal gravity waves propagating at an angle to the jet axis undergo resonance superreflection at the velocity shear surface made up of the jet boundaries;
- the harmonics of internal gravity waves resonate between the jet boundaries and propagate inside the jet like in a waveguide; during this process, the energy of gravity waves increases with time, amplified via superreflection (resonance waveguide instability);
- the development of instability results in the formation of a system of nonlinear waves around the jet, which heat up the ambient medium; it is important that the wave resistance of the ambient medium is significantly higher than that of the jet matter and therefore the heating mentioned above occurs inside a cone with a limited opening angle (which depends on particular parameters of the system) around the jet;
- the allowance for the possible nonlinear superposition of different modes and projection effects permits obtaining the qualitative pattern of the observed morphology of real objects and of the velocity field inside the ionization cones.

As far as we know, no one has yet explored the possibility of the development of the above modes, unlike the unstable acoustic modes of jets emerging from young stellar objects, which were studied by a number of authors (see Ferrari et al., 1982; Payne & Cohn, 1985; Hardee & Norman, 1988; Norman & Stone, 1997; Norman & Hardee, 1988). In this paper, we show the principal possibility of the buildup of both helical and pinch waveguide-resonance internal gravity modes in conic jets, and discuss the results of nonlinear numerical modeling of this process.

In Section 2 we describe the equilibrium model employed; in Section 3 we give the linearized equations and formulate the problem of determining the eigenfrequencies of unstable jet modes; in Section 4 we discuss the dispersion of perturbations during the linear stage of instability, and in Section 5 we summarize the main conclusions and make the final comments. We analyze the results of nonlinear 2D- and 3D-modeling in our next paper (Afanasiev et al., 2007, hereafter referred to as Paper II).

## 2. Equilibrium model

Analyses of the dynamics of jet outflows from active galactic nuclei naturally reveal three characteristic regions in radial coordinate  $r$ :

- at  $r < (1 - 10)$  pc the gravitational field is determined mostly by the Newtonian potential of the central massive object;
- at  $(1 - 10) \leq r \leq (500 - 1000)$  pc the jet is immersed in dispersed mass of the stellar bulge, which can be considered to be spheroidal to a first approximation. This region coincides with the rigid-rotation region of the galactic disk (Sofue & Rubin, 2001) and therefore the gravitational potential can be assumed to be proportional to squared radius to a fair accuracy;

- at  $r > (0.5 - 1)$  kpc the variation of the gravitational potential along the jet outflow differs substantially for different galaxies. Moreover, it also strongly depends on the orientation of the jet relative to the symmetry plane of the galactic disk.

In this paper we analyze the spectrum of unstable modes of a jet located in the gravitational field with potential  $\Psi \propto r^2$ . Note that wave structures that form in the jet in the inner part of the galaxy, where potential can be fitted fairly well by the Newtonian formula, are incapable of distorting the wave pattern over the jet region considered. First, because the radial wavelength of perturbations in the field of a point mass must decrease with distance from the gravitating center,  $\lambda_r \propto r^{-1/2}$  (Levin et al., 1999), and the spatial scale length is incomparable with the characteristic wavelength. Second, according to Levin et al. (1999), the jet region, where energy can be fed to perturbations via resonance superreflection and hence where wave structures with appreciable amplitudes can exist, has a limited extent.

Our aim is to find out whether it is in principle possible for unstable modes to develop at the layer between the jet and the ambient medium, and therefore we do not incorporate the galactic disk into our equilibrium model. We show in our next paper (Paper II) that in the case of  $\Psi(r) \propto r^2$  perturbations in the ambient medium are localized in the conic domain near the jet. Hence our formulation of the problem is formally correct, at least for Seyfert galaxies with powerful bulges and ionization cones lying outside the plane of the galactic disk.

We perform our analysis in the spherical coordinate system  $(r, \theta, \varphi)$ , where the  $\theta = 0$  axis coincides with the symmetry axis of the jet with an opening angle of  $\theta_j$  and outflow velocity of  $\mathbf{V} = V_j \mathbf{e}_r$ . Here  $\mathbf{e}_r$  is the unit basis vector. We model the medium by ideal gas with the following equation of state

$$p_i = c_i^2 \rho_i / \gamma, \quad (1)$$

where  $p_i$  and  $\rho_i$  are the unperturbed (equilibrium) pressure and density, respectively;  $c_i$  is the adiabatic sound speed; subscript  $i$  is equal to “ $j$ ” and “ $a$ ” inside and outside the jet, respectively; we assume that adiabatic index  $\gamma$  is the same for the matter of the jet and the ambient gas. We assume that gravitational field is spherically symmetric with the center located at the coordinate origin. Variations of the gravitational potential can be written in the following form:

$$\Psi = \Psi_0 + \frac{1}{2} \Omega^2 r^2, \quad (2)$$

where  $\Omega = \text{const}$  is the angular velocity of gas rotation in the circumnuclear region of the disk and  $\Psi_0 = \text{const}$  is a normalizing constant.

We assume that gas outside the jet is at rest. We take into account the possible heating of gas of the jet by the radiation of the nucleus:  $q_j > 0$ , where  $q_j = \Gamma - \rho_j \Lambda$  is the amount of energy absorbed by unit mass per unit

time;  $\Gamma = \Gamma(T)$  and  $\Lambda = \Lambda(T)$  are the heating and cooling functions, respectively, which depend on temperature  $T$  exclusively. In the equilibrium state  $q_a = 0$  outside the jet.

Thus the spatial distribution of the model parameters that characterize unperturbed flow has the following form:

$$V; \rho; c; q = \begin{cases} 0; \rho_a(r); c_a(r); 0, & \theta > \theta_j \\ V_j(r); \rho_j(r); c_j(r); q_j(r), & \theta < \theta_j \end{cases} \quad (3)$$

We assume that the jet is contained by the pressure of ambient gas and hence that the following equality is satisfied at  $\theta = \theta_j$ :

$$\rho_j(r)c_j^2(r) = \rho_a(r)c_a^2(r). \quad (4)$$

Note that below we make virtually no direct use of relation (4), its fulfillment is required for realization of a flow with  $V_\theta \equiv 0$ .

Radial dependences in formula (3) are determined first and foremost by the unperturbed balance of forces. Under the adopted assumptions, the  $r$  component of Euler's equations implies

$$\frac{1}{2} \frac{\partial V_i^2}{\partial r} + \Omega^2 r = -\frac{1}{\rho_i} \frac{\partial p_i}{\partial r}. \quad (5)$$

It follows from the continuity equation that

$$\rho_j V_j = \dot{\mu}_j / r^2. \quad (6)$$

In equation (6)  $\dot{\mu}_j = \text{const}$  is the mass-loss rate by the system into a unit steradian. It is a free parameter of our model.

Finally, in the case considered the equation of energy balance, with formulas (1) and (6) taken into account, can be written in the following form:

$$V_i \frac{\partial}{\partial r} \left( \frac{V_i^2}{2} + \frac{c_i^2}{\gamma - 1} \right) + \Omega^2 r V_i = q_i. \quad (7)$$

Equation of state (1) closes equation set (4)–(7).

We seek the solutions of this equation set in the power-law form:  $f(r) \propto r^{\alpha_f}$ , where  $f$  is any of the parameters that characterize the system. It follows from equation (5), with equation (1) taken into account, that  $\alpha_V V_i^2 + \Omega^2 r^2 = -\alpha_p c_i^2 / \gamma$ . Hence we find:

$$\alpha_V = \alpha_c = 1, \quad \alpha_p = -3, \quad \alpha_q = -1, \quad \alpha_q = 2. \quad (8)$$

In this case, for a spherically symmetric potential the velocity of matter in the jet relates to the sound speed in the ambient medium as:

$$V_j^2 = \frac{1}{\gamma} (c_j^2 - c_a^2). \quad (9)$$

The Mach number of the jet is  $M = V_j / c_j < 1$ , i.e., the jet is subsonic. Note that this condition can be satisfied simultaneously with  $V_j / c_a \gg 1$ , making it theoretically possible for shocks due to the development of instability at the jet boundary to exist in the medium that surrounds the jet, because  $c_a < c_j$ .

Given that  $\gamma > 1$ , our model corresponds to an entropy distribution  $S_i$  that is stable against convective motions, because

$$\frac{dS_i}{dr} = \frac{\rho_i^\gamma}{p_i} \frac{d}{dr} \left( \frac{p_i}{\rho_i^\gamma} \right) = \frac{\alpha_p - \gamma \alpha_\rho}{r} = \frac{3\gamma - 1}{r} > 0. \quad (10)$$

Substitution of power-law radial dependences into formulas (5) and (7) and comparison with formula (9) yield:

$$V_j = \frac{\gamma(\gamma - 1)}{3\gamma - 1} \frac{r q_j}{c_j^2}. \quad (11)$$

Hence the velocity of matter in the jet is unambiguously determined by its temperature and heating due to external radiation. Heating is rather important for outflows emerging from active galactic nuclei, because the jet is illuminated intensively by the radiation of the nucleus.

We finally determine, in view of formula (8), that the following condition must be satisfied for the realization of the model constructed above:

$$\Gamma(\varepsilon_i) = C_\Gamma \varepsilon_i, \quad \Lambda(\varepsilon_i) = C_\Lambda \varepsilon_i^{5/2}. \quad (12)$$

Here  $C_\Gamma$  and  $C_\Lambda$  are constants and  $\varepsilon_i$  is the internal energy of gas. For further calculations, it is more convenient to write heating and cooling in terms of internal energy, and not in terms of temperature, by taking advantage of the fact that  $(\gamma - 1)\varepsilon = RT/\mu$  for ideal gas. Note that in the temperature interval  $T < 10^6$  the second relation in (12) agrees excellently with the dependence  $\Lambda(T) \propto T^{2.53}$  that is typical of ionized gas in Seyfert galaxies (MacDonald & Bailey, 1981; Norman & Stone, 1997). Linear temperature dependence of heating function  $\Gamma$  in formula (12) is also a good approximation.

### 3. Linearized equations and formulation of the boundary-value problem

Let us now analyze the stability of the model that we constructed in the previous section against small perturbations. We proceed from the following set of hydrodynamics equations:

$$\frac{\partial \mathbf{V}}{\partial t} + (\mathbf{V} \nabla) \mathbf{V} = -\frac{1}{\rho} \nabla p - \nabla \Psi, \quad (13)$$

$$\frac{\partial \rho}{\partial t} + (\mathbf{V} \nabla) \rho + \rho \operatorname{div} \mathbf{V} = 0, \quad (14)$$

$$\frac{\partial \varepsilon}{\partial t} + (\mathbf{V} \nabla) \varepsilon + (\gamma - 1) \varepsilon \operatorname{div} \mathbf{V} = C_\Gamma \varepsilon - C_\Lambda \rho \varepsilon^{5/2}. \quad (15)$$

We obtain the missing equation to close this set by choosing the equation of state in the form  $p = p(\rho, S)$  and computing its derivative with respect to time:

$$\begin{aligned} \frac{dp}{dt} &= \left( \frac{\partial p}{\partial \rho} \right)_S \frac{d\rho}{dt} + \left( \frac{\partial p}{\partial S} \right) \frac{dS}{dt} = \\ &= c_i^2 \frac{d\rho}{dt} + \frac{p_i}{c_v} \frac{dS}{dt} = c_i^2 \frac{d\rho}{dt} + (\gamma - 1) \rho_i \frac{T_i}{T} q. \end{aligned} \quad (16)$$

Our computations take into account the fact that  $S = c_v \ln(p/\rho^\gamma)$ ,  $c_p - c_v = R/\mu$ ,  $\gamma = c_p/c_v$ ,  $dS/dt = q/T$ , and use the equation of state of ideal gas in the form  $p = R\rho T/\mu$ .

Thus the last equation of the above set acquires the following form:

$$\frac{\partial p}{\partial t} + (\mathbf{V}\nabla)p = c_i^2 \left[ \frac{\partial \rho}{\partial t} + (\mathbf{V}\nabla)\rho \right] + (\gamma - 1)\rho_i \varepsilon_i (C_\Gamma - C_\Lambda \rho \varepsilon_i^{3/2}). \quad (17)$$

To avoid doubts, note that subscript “ $i$ ” indicates equilibrium stationary parameter values.

We now use standard procedure of linear analysis to substitute pressure, internal energy, density, and velocity of the medium in the form  $f(r, \theta, \varphi, t) = f_i(r) + \tilde{f}(r, \theta, \varphi, t)$ , where  $|\tilde{f}| \ll f_i$ . We assume that conditions (5)–(7) are satisfied to derive the following set of equations describing the dynamics of small nonadiabatic perturbations written for domains that are homogeneous in  $\theta$ :

$$\frac{\partial \tilde{v}_r}{\partial t} + V_i \frac{\partial \tilde{v}_r}{\partial r} + \tilde{v}_r \frac{\partial V_i}{\partial r} = -\frac{1}{\rho_i} \frac{\partial \tilde{p}}{\partial r} + \frac{\tilde{\rho}}{\rho_i^2} \frac{\partial p_i}{\partial r}, \quad (18)$$

$$\frac{\partial \tilde{v}_\theta}{\partial t} + V_i \frac{\partial \tilde{v}_\theta}{\partial r} + \frac{V_i \tilde{v}_\theta}{r} = -\frac{1}{\rho_i r} \frac{\partial \tilde{p}}{\partial \theta}, \quad (19)$$

$$\frac{\partial \tilde{v}_\varphi}{\partial t} + V_i \frac{\partial \tilde{v}_\varphi}{\partial r} + \frac{V_i \tilde{v}_\varphi}{r} = -\frac{1}{\rho_i r \sin \theta} \frac{\partial \tilde{p}}{\partial \varphi}, \quad (20)$$

$$\frac{\partial \tilde{\rho}}{\partial t} + \frac{1}{r^2} \frac{\partial}{\partial r} [r^2 (\tilde{\rho} V_i + \rho_i \tilde{v}_r)] + \frac{1}{r \sin \theta} \left[ \frac{\partial}{\partial \theta} (\rho_i \tilde{v}_\theta \sin \theta) + \frac{\partial}{\partial \varphi} (\rho_i \tilde{v}_\varphi) \right] = 0, \quad (21)$$

$$\frac{\partial \tilde{p}}{\partial t} + V_i \frac{\partial \tilde{p}}{\partial r} + \tilde{v}_r \frac{\partial p_i}{\partial r} = c_i^2 \left( \frac{\partial \tilde{\rho}}{\partial t} + V_i \frac{\partial \tilde{\rho}}{\partial r} + \tilde{v}_r \frac{\partial \rho_i}{\partial r} \right) - p_i C_\Lambda \left( \varepsilon_i^{3/2} \tilde{\rho} + \frac{3}{2} \varepsilon_i^{1/2} \rho_i \tilde{\varepsilon} \right), \quad (22)$$

$$\frac{\partial \tilde{\varepsilon}}{\partial t} + V_i \frac{\partial \tilde{\varepsilon}}{\partial r} + \tilde{v}_r \frac{\partial \varepsilon_i}{\partial r} + \left[ (\gamma - 1) \frac{\partial V_i}{\partial r} - (\gamma + 1) \frac{V_i}{r} + \frac{3}{2} C_\Lambda \rho_i \varepsilon_i^{3/2} \right] \tilde{\varepsilon} + (\gamma - 1) \varepsilon_i \left[ \frac{\partial \tilde{v}_r}{\partial r} + \frac{2\tilde{v}_r}{r} + \frac{1}{r \sin \theta} \left( \frac{\partial (\tilde{v}_\theta \sin \theta)}{\partial \theta} + \frac{\partial \tilde{v}_\varphi}{\partial \varphi} \right) \right] = -C_\Lambda \varepsilon_i^{5/2} \tilde{\rho}. \quad (23)$$

We take equation (11) into account when deriving formula (23) from formula (15).

We seek the solutions for perturbed quantities in the following form:

$$\tilde{f}(r, \theta, \varphi, t) = \hat{f}(\theta) r^{\beta_f} \exp \{i\chi(r, t) + im\varphi\}. \quad (24)$$

Based on the requirement of conservation of the flux of perturbation energy through a sphere of arbitrary radius ( $r^2 \tilde{p} \tilde{v}_r = \text{const}$ ), we find the exponent of the radial dependences of perturbation amplitudes to be  $\beta_f = \alpha_f - \alpha_\Psi/2$ . Here  $\alpha_f$  is, as above, the exponent for equilibrium quantities, and  $\alpha_\Psi = 2$ , the exponent for the gravitational potential (2). It is important that for this  $\alpha_\Psi$  value formula (24)

gives exact solutions. Let us now introduce the following designations:  $k = \partial\chi/\partial r$ ,  $\omega = -\partial\chi/\partial t$ . In this case, equation set (18)–(23) for the equilibrium model considered reduces to the following two ordinary differential equations:

$$\frac{d\hat{p}}{d\theta} = \hat{\omega}_i (\hat{\omega}_i + \delta_i) \rho_i r^3 \hat{\xi}, \quad (25)$$

$$\frac{d\hat{\xi}}{d\theta} = \frac{1}{r \hat{\omega}_i (\hat{\omega}_i + \delta_i)} \left[ \lambda_i + \frac{m^2}{r^2 \sin^2 \theta} \right] \frac{\hat{p}}{\rho_i} - \hat{\xi} \cot \theta. \quad (26)$$

Here  $\hat{\omega}_i = \omega - kV_i$  is the Doppler shifted perturbation frequency and  $\delta_i = iV_i/r$ ,  $\hat{\xi}$  is the complex amplitude of perturbed Lagrangian  $\theta$ -displacement of the medium such that:

$$\tilde{v}_\theta = \frac{d\tilde{\xi}}{dt} = -i(\omega - kV_i)\tilde{\xi} = -i\hat{\omega}_i \tilde{\xi}. \quad (27)$$

We introduced the following designation in formula (26):

$$\lambda_i = \left( k + \frac{i}{r} \right) \left( k + \frac{2i}{r} \right) - \left[ \rho_i (\hat{\omega}_i^2 - \delta_i^2) + \frac{i}{r} (k + \frac{i}{r}) p_i \right] \times \left[ \frac{\hat{\omega}_i - 2\delta_i}{p_i} + \frac{i\hat{A}_\Lambda (3\gamma - 1)(k + \frac{2i}{r})}{r \rho_i (\hat{\omega}_i + \delta_i)} \right] \times \left\{ \hat{\omega}_i - (3\gamma + 1)\delta_i + \hat{A}_\Lambda \left[ (\gamma - 1)(\hat{\omega}_i - \delta_i) - iC_\Lambda \rho_i \varepsilon_i^{3/2} - \frac{3\gamma - 1}{\gamma r^2} \frac{c_i^2}{\hat{\omega}_i + \delta_i} \right] \right\}^{-1}, \quad (28)$$

where

$$\hat{A}_\Lambda = 1 - \frac{\frac{3}{2} i C_\Lambda \rho_i \varepsilon_i^{3/2}}{\hat{\omega}_i - \delta_i + \frac{3}{2} i C_\Lambda \rho_i \varepsilon_i^{3/2}}.$$

To solve the boundary-value problem for the determination of unstable-mode eigenfrequencies, four boundary conditions must be satisfied. We use standard boundary conditions at the jet axis based on the physical assumptions of Hardee & Norman (1988) and Norman & Hardee (1988). All displacements for axisymmetric perturbations should be equal to zero at the jet axis,  $\hat{\xi}(0) = 0$ . In the case of nonaxisymmetric perturbations ( $m > 0$ ) the term with  $\hat{p}(0)$  in formula (26) is finite along the jet axis only for  $\hat{p}(0) \equiv 0$ . Hence:

$$\begin{cases} \hat{p}(0) = 0, & m \geq 1, \\ \hat{\xi}(0) = 0, & m = 0, \end{cases} \quad (29)$$

$$\begin{cases} \hat{p}(\pi) = 0, & m \geq 1, \\ \hat{\xi}(\pi) = 0, & m = 0, \end{cases} \quad (30)$$

To find the boundary conditions at the external ( $\theta = \theta_j$ ) jet boundary, we integrate equations (25) and (26) from  $\theta_j - \varepsilon$  to  $\theta_j + \varepsilon$  (where  $\varepsilon \rightarrow 0$ ). Here we adopt  $\rho_i(\theta) = \rho_j - (\rho_j - \rho_a)\hat{\theta}(\theta - \theta_j)$ , where  $\hat{\theta}(\theta - \theta_j)$  is the symmetric Heaviside step function. In the same way we determine  $V_i(\theta)$ ,  $p_i(\theta)$ ,  $\varepsilon_i(\theta)$ , and  $c_i(\theta)$ . Integration yields the following conditions:

$$\hat{p}(\theta_j - 0) = \hat{p}(\theta_j + 0), \quad (31)$$

$$\hat{\xi}(\theta_j - 0) = \hat{\xi}(\theta_j + 0), \quad (32)$$

because the right-hand sides in equations (25) and (26) contain no  $\delta$ -functions (i.e., derivatives of  $\theta$ -functions). From the physical viewpoint this means the continuity of total pressure ( $p_i + \tilde{p}$ ) at the jet boundary bended by perturbations (with the allowance for equation (4)) and the absence of cross-boundary gas flows.

The dispersion properties of small perturbations in the system considered are fully characterized by the following dimensionless parameters:

- constant Mach number  $M = V_j/c_j$  along the jet;
- density difference between the ambient gas and jet matter  $\tilde{R} = \rho_a/\rho_j = c_j^2/c_a^2$ ;
- radius-independent fractional radial wavenumber  $kr$ ;
- helical-mode number (the number of spiral arms in azimuth)  $m$ ;
- the ratio of the acoustic wave period to the relaxation time scale of the gas of the jet  $\tau = C_\Lambda \rho_j c_j^{3/2}/kc_j$ ;
- dimensionless phase velocity of perturbations along the jet axis  $z = \omega/kc_j$ , which is a solution of equation set (25)–(26) with boundary conditions (29)–(32). In this case,  $z$  is also radius independent.

The condition of growth of fractional perturbation amplitude ( $Im z > 0$ ) means that the mode considered is unstable.

Only one of the two parameters —  $M$  and  $\tilde{R}$  — is independent, whereas the second parameter can be computed by relation (9):  $M^2 = (1 - 1/\tilde{R})/\gamma$ . We further assume, for the sake of simplicity, that gas has the same composition throughout the entire system, implying that the external cooling coefficient  $\tau_a$  is related to the cooling coefficient in the jet as  $\tau = \sqrt{\tilde{R}} \tau_a$ .

Note that in the case of fixed medium with no radiative cooling ( $V_i = 0$ ,  $C_\Lambda = 0$ ,  $\delta_i = 0$ ,  $\hat{\omega}_i = \omega$ ) we set  $\tilde{v}_\theta \equiv 0$ ,  $m = 0$  to immediately derive from the linearized equation set for perturbations with wave vector  $\mathbf{k} \parallel \mathbf{e}_r$  the following dispersion equation, which is equivalent to  $\lambda_i = 0$  in equation (26). Its solution has the form:

$$\omega = \pm kc_i \sqrt{1 + \frac{4\gamma - 1}{\gamma k^2 r^2}}. \quad (33)$$

Thus in the short-wavelength approximation ( $kr \gg 1$ ) we obtain the common dispersion law for acoustic waves:  $\omega \simeq \pm kc_i$ . The opposite limiting case  $kr \ll 1$  leads to the following dispersion relation:

$$\omega \simeq \pm \sqrt{\frac{4\gamma - 1}{\gamma}} \frac{c_i}{r}. \quad (34)$$

Relation (34) describes the dispersion law for long-wavelength gravity waves.

## 4. Discussion of the results of linear analysis

### 4.1. Medium Without Relaxation

To make it easier to identify the causes of the development of unstable modes, we first consider the case of

a medium without relaxation:  $\tau \equiv 0$  (adiabatic perturbations). We use the shooting method to solve numerically the boundary-value problem formulated in Chapter 3. Figs. 2–4 show the resulting dispersion curves. The spectrum of unstable modes is discrete and rather complex.

First, the surface modes resulting from the development of the Kelvin–Helmholtz instability (KHI) in the domain of tangential velocity discontinuity between the jet and the ambient medium. These modes decay exponentially with the distance from the jet boundary on both sides in the  $\theta$ -coordinate.

Second, the modes of the waveguide made up of the jet boundary, which are characterized by two “quantum” numbers —  $n_j$  and  $m$ . Here  $n_j$  is the number of nodes of the eigenfunctions of perturbed pressure between the boundary of the jet and its symmetry axis determined in the direction perpendicular to this axis and  $m$  is the number of zero points along the jet azimuth (the number of arms of the helical spiral in the cross section of the jet). Axisymmetric modes with  $m = 0$  are called pinch modes and nonaxisymmetric modes are called  $m$ -helical modes according to the number of zero points in azimuth. The harmonics with no zero points along the jet radius are the main harmonics and the remaining ones are reflective harmonics.

Third, the spectrum of modes contains weakly unstable or decaying ( $Im \omega < 0$ ) harmonics. For these modes a change of any parameter has no effect on the number of zero points (i.e., the  $n_a$  of this function in the medium surrounding the jet) of the  $\theta$  distribution of perturbed pressure between the jet boundary and the  $\theta = \pi$  axis, whereas the number  $n_j$  of zero points for the jet does change. Such modes are a direct consequence of the idealized formulation of the problem, because the ambient medium can also be formally viewed as a waveguide. However, in the real situation the development of a standing wave in  $\theta$  coordinate between the jet boundary and the  $\theta = \pi$  axis shall be impeded by local heterogeneities present.

In the situation considered the dispersion properties of perturbations differ substantially from those in the case of the gravitational potential of a compact object. This is due, first and foremost, to weak compressibility of the medium in the jet on the one hand, and to appreciable density stratification on the other hand.

The local dispersion law allows the existence of two types of oscillatory modes in each of these media. These are gravity acoustical waves (GAW) and internal gravity waves (IGW). GAWs are common longitudinal acoustic waves modified by gradient effects. IGWs are due to the shear elasticity of the medium resulting from the disbalance of buoyancy and gravity forces. In the limiting case of incompressible medium ( $M \ll 1$ ) they become transverse waves.

Our model has a preferred direction — that of the velocity shear vector, which is parallel to the gravity force, — and therefore for each of these types of modes one can single out waves propagating in the direction of the velocity shear and in the opposite direction. Therefore, as is

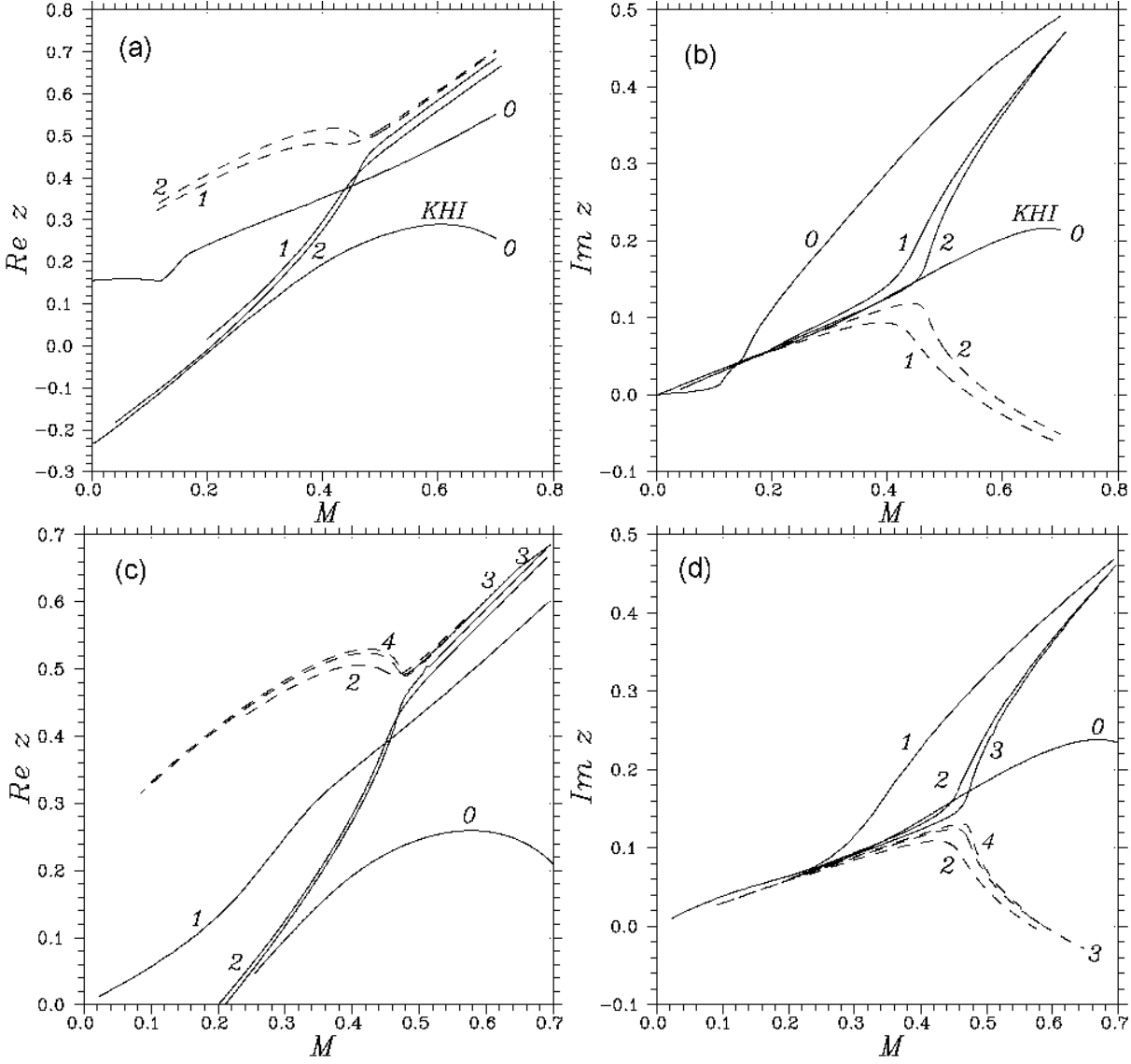


**Fig. 2.** Dimensionless phase velocity  $Re(\omega/kc_j)$  (a, c) and amplitude increments  $Im(\omega/kc_j)$  (b, d) as functions of the Mach number  $M = V_j/c_j$  for axisymmetric (a, b) and helical  $m = 1$  unstable modes (c, d). The number  $n_j$  of zero points of eigenfunctions inside the jet is indicated near each curve. The jet half-opening angle is equal to  $\theta_j = 20^\circ$ ,  $kr = 5$ . The dashed and solid lines show the  $u^+$  and  $u^-$  mode families, respectively.

evident from Fig. 2a,c, all modes break into two families: in the reference frame connected with matter modes of one family ( $u^+$ ) propagate away from the ejection source and modes of the other family ( $u^-$ ) propagate toward the source. In the case of a medium with no radiative cooling all these modes turn out to be unstable over a wide range of parameters.

One can determine that most of the dispersion curve shown in Fig. 2 corresponds to IGW by directly comparing our results with the solution of the well-known problem of wave dispersion in a compressible medium with vertical density stratification due to uniform gravity field  $-g\mathbf{e}_z$ .

The short-wavelength approximation of the corresponding dispersion equation has the following form (see Appendix):

$$\begin{aligned} \hat{\omega}^4 + \left[ g \frac{d \ln \rho_0}{dz} - (k_z^2 + k_\perp^2) c_s^2 \right] \hat{\omega}^2 \\ - g k_\perp^2 \left( g + c_s^2 \frac{d \ln \rho_0}{dz} \right) = 0, \end{aligned} \quad (35)$$

where  $\hat{\omega} = \omega - \mathbf{kV}$ ,  $k_\perp^2 = k_x^2 + k_y^2$ .

We now use the short-wavelength approximation to make the formal transition from equation (35) to the case considered by substituting the  $r$  coordinate for the  $z$  coordinate,  $k$  for  $k_z$ ,  $k_\perp^2 = k_\theta^2 + m^2/r^2$  for  $k_\perp^2$ ,  $\rho_i$  for  $\rho_0$ ,  $c_i$  for  $c_s$ , and  $p_i$  for  $p_0$ . Given the power-law behavior of the dependences of thermodynamic parameters with exponents (8), we normalize equation (35) by  $k^4 c_i^4$  to find the local

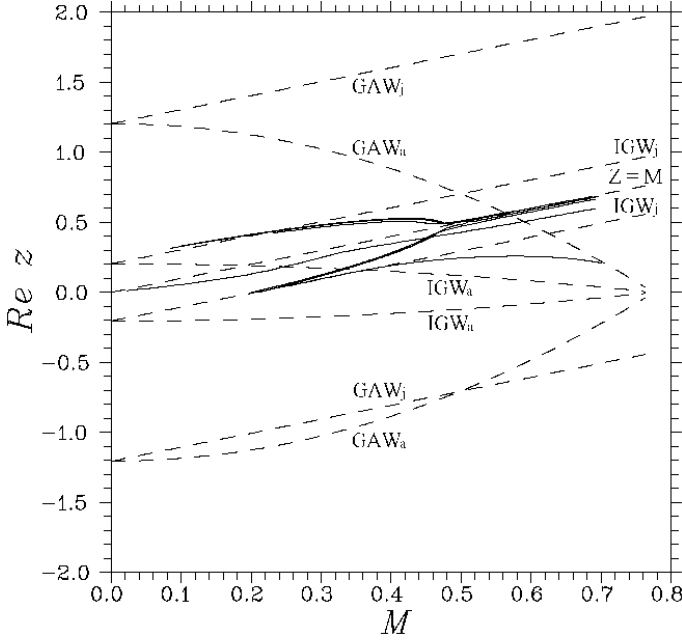


**Fig. 3.** Dispersion curves from Fig. 2a (solid curves), gravity-acoustic (GAW) and internal gravity (IGW) eigenmodes of the jet and atmosphere determined from eq. (36), (37) (dashed curves).

dimensionless dispersion laws for the ambient medium and jet, respectively:

$$(z - M)^4 - \left(1 + \delta^2 + \frac{3}{\gamma k^2 r^2}\right)(z - M)^2 + \frac{\delta^2}{\gamma^2 k^2 r^2}(3\gamma - 1) = 0, \quad (36)$$

$$(\tilde{R}z)^4 - \left(1 + \delta^2 + \frac{3}{\gamma k^2 r^2}\right)(\tilde{R}z)^2 + \frac{\delta^2}{\gamma^2 k^2 r^2}(3\gamma - 1) = 0. \quad (37)$$

Parameter  $\delta = k_{\perp}/k$  characterizes the inclination of the perturbation propagation vector with respect to the radial direction.

Figure 3 shows all solutions of equations (36)–(37), the straight line  $z = M$  corresponding to the velocity of the jet matter, and the dispersion curves from Fig. 2a. It is evident that the dispersion curves of our jet modes tend to the curves corresponding to IGWs.

Like in the case of jets emerging from young stellar objects (Ferrari et al., 1982; Payne & Cohn, 1985; Hardee & Norman, 1988; Norman & Hardee, 1988), instability in our case is due to superreflection and superrefraction (Miles, 1957; Ribner, 1957).

Flow in the jet is subsonic in our model. However, the excess of velocity shear at the jet boundary over the wave velocity along this boundary, which is required for superreflection, is achieved owing to the smallness of the characteristic propagation velocity of internal gravity waves. For the parameter values corresponding to the curves shown in Figs. 2–4 this corresponds to an  $\simeq 0.2$  increase

in the Mach number. Thus the allowance for gravity results in the appearance of additional unstable jet modes — waveguide-resonance internal gravity waves whose amplification mechanism is due to the superreflection of this type of waves from the jet boundary.

Because of their low Mach numbers, gravity-acoustic waves do not satisfy the superreflection condition. In this case the main physical cause of instability is the Bernoulli effect — the well-studied Kelvin–Helmholtz instability develops at the velocity-shear layer between the jet matter and the surrounding gas. At the same time, these waves resonate between the jet boundary and the  $\theta = \pi$  axis and the process is accompanied by the formation of a weakly unstable wave in the case of a medium without relaxation.

The amplitude increment of each reflective harmonic ( $n_j \geq 1$ ) grows rapidly with decreasing radial wavenumber (see Fig. 4). However, this is not a physical effect, but only a result of normalization by  $kc_j$ . It becomes clear below (see 4.2) that renormalization to the wavenumber independent Väisälä frequency results in the unlimited decrease of the growth time scale of unstable IGW modes with decreasing radial wavelength.

An important result is that the time scales of the development of the instability discussed here depend only slightly on the jet opening angle (see Fig. 5).

The extremely weak dependence of the increments of unstable modes on jet parameters leads us to suggest that different modes may develop simultaneously and coexist. On the other hand, we can conclude that the wavelengths at which the instability builds up, should be to a greater degree determined by the initial perturbations.

At the same time, the amplitude increment of reflective harmonics decreases and that of the main harmonics ( $n_j = 0$ ) — both the axisymmetric and the first helical modes of internal gravity waves — on the contrary, increases with increasing  $kr$ . Moreover, at  $kr \geq 10$  these modes are most likely to develop instability.

#### 4.2. Effect of Radiative Cooling on the Dispersion of Unstable Modes

The allowance for radiative losses changes radically the spectrum of unstable modes in the system considered:

**GAW modes** are completely suppressed by radiative cooling and their decay decrements exceed the frequency by a factor of several tens to several hundred. This actually means that such modes cannot even develop. We therefore do not show the corresponding dispersion curves in our figures in order not to encumber them.

**Surface KHI modes** are extremely sensitive to radiative cooling. Their growth time scale increases only slightly compared to the case of adiabatic perturbations (see Figs. 6–7).

**Waveguide-resonance modes of IGW of the  $\mathbf{u}^+$  family** become damped already at small values of radiation-cooling parameter  $\tau$ . Their damping time scale decreases rapidly with increasing  $\tau$  (see Fig. 7b). It can

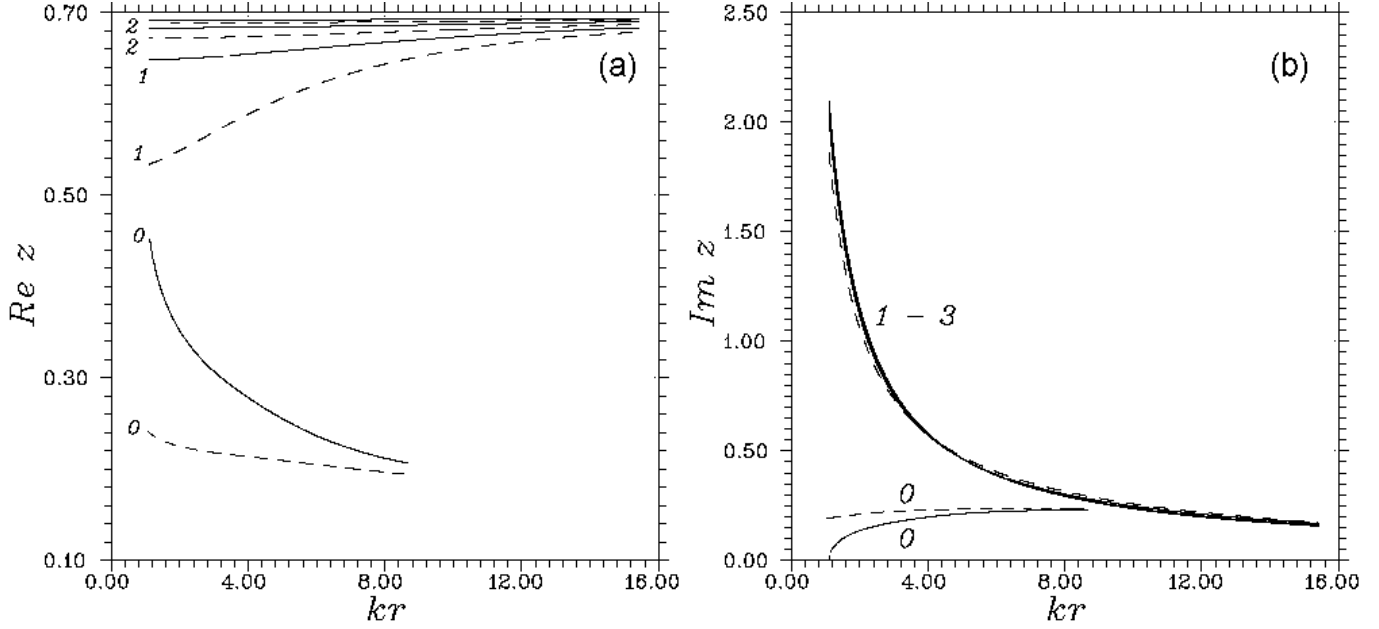


**Fig. 4.** Dependences of dimensionless phase velocity  $Re(\omega/kc_j)$  (a) and fractional growth rate of the amplitude of unstable modes  $Im(\omega/kc_j)$  (b) on dimensionless wavenumber  $kr$ . The solid and dashed curves show the modes with  $m = 0$  and  $m = 1$ , respectively. The number of zero points of eigenfunctions inside the jet is indicated near each curve. The half-opening angle of the jet is  $\theta_j = 20^\circ$ ,  $M = 0.7$ .

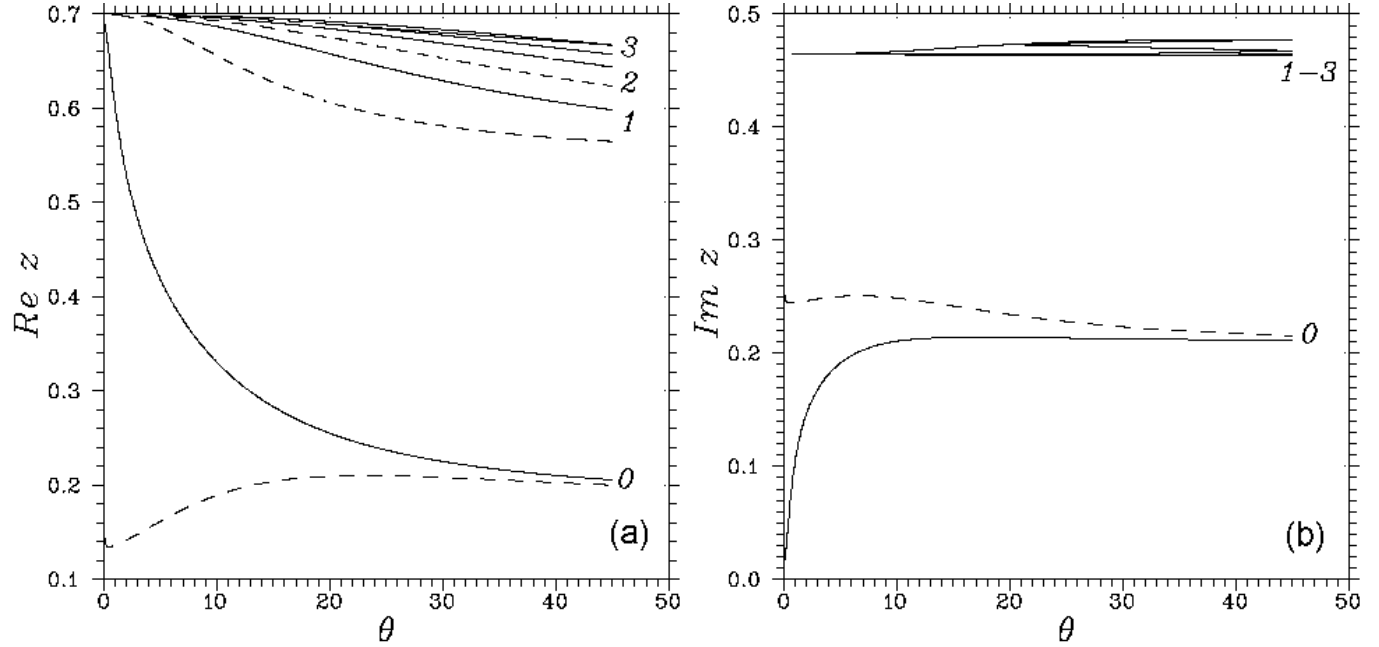


**Fig. 5.** Dimensionless phase velocities  $Re(\omega/kc_j)$  (a) and amplitude increments  $Im(\omega/kc_j)$  (b) as functions of the jet half-opening angle  $\theta_j$  in degrees. Designations are the same as in Fig. 4.  $kr = 5$ ,  $M = 0.7$ .

therefore be argued that they are also fully suppressed by radiative cooling. We show the dispersion curves corresponding to these modes only in Fig. 7. Note that strictly speaking, in the presence of radiative cooling these modes should be called entropy-vortex-type and not internal gravity modes. We nevertheless retain the old name to facilitate the comparison to the case of the medium without relaxation.

**Waveguide-resonance IGW modes of the  $u^-$  family** increase in strength substantially because of radiation losses. Their increment increases with increasing  $\tau$  (Fig. 7) without reaching saturation<sup>1</sup>.

To explain the latter effect, we must use the formula relating wave energy density  $E$  in a moving medium to

<sup>1</sup> We verified this statement by computations up to  $\tau = 100$

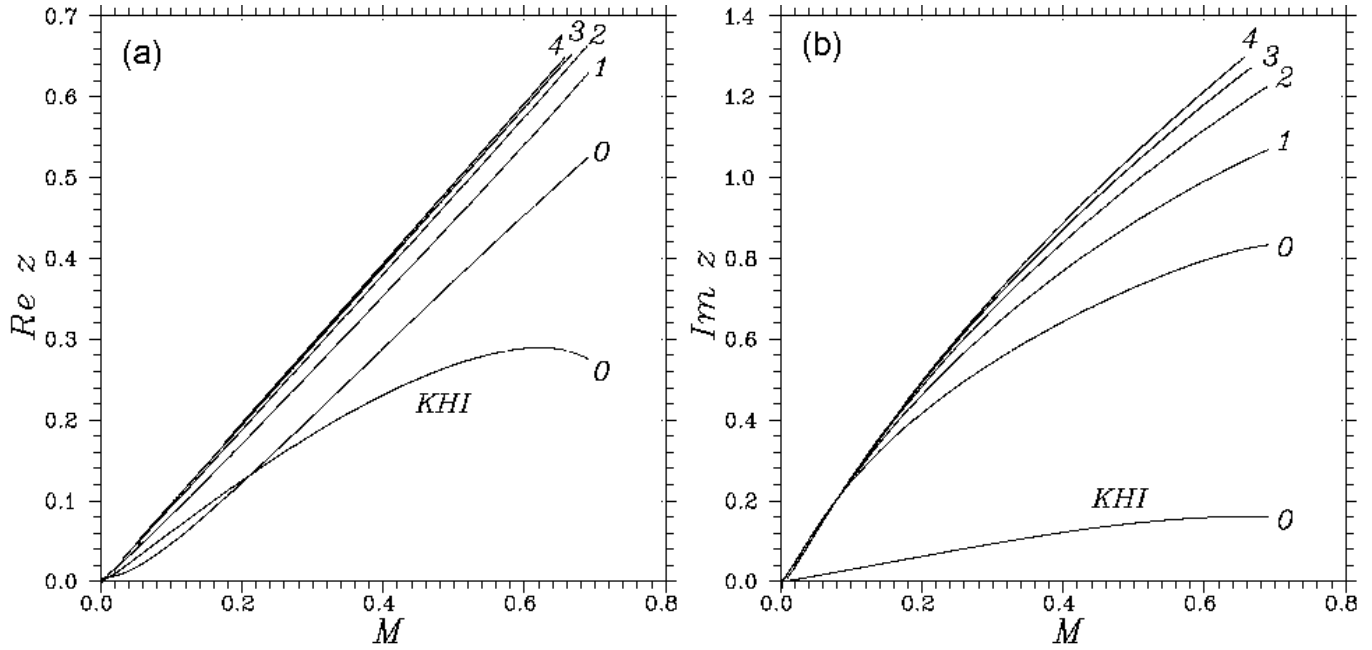


**Fig. 6.** Dimensionless phase velocities  $Re(\omega/kc_j)$  (a) and amplitude increments  $Im(\omega/kc_j)$  (b) as functions of the Mach number for modes with radiative cooling ( $\tau = 5$ ). Each curve is labelled by the number of the harmonic (the number of zero points of pressure between the boundary and the jet axis). Only  $u^+$ -family harmonics of mode  $m = 0$  are shown.  $\theta_j = 20^\circ$ ,  $kr = 5$ .

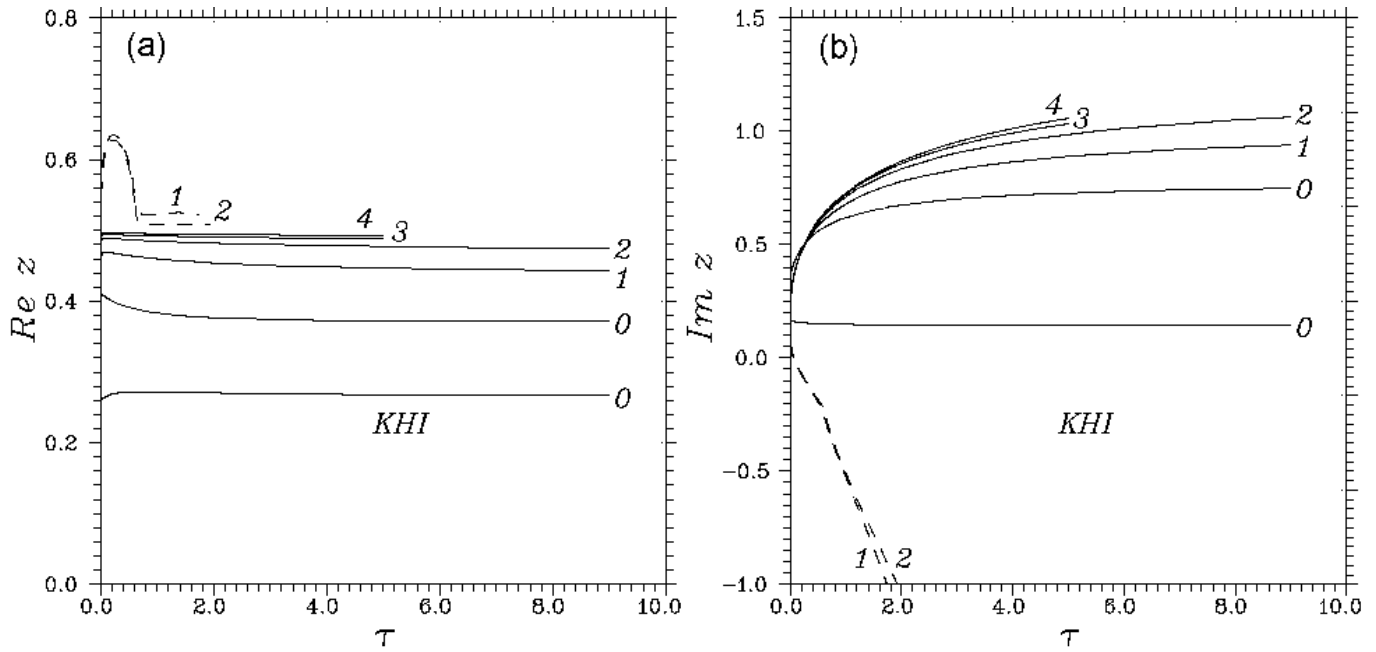


**Fig. 7.** Dimensionless phase velocities  $Re(\omega/kc_j)$  (a) and amplitude increments  $Im(\omega/kc_j)$  (b) as functions of radiative-cooling parameter  $\tau$  for different unstable modes. Each curve is labelled by the number of the harmonic (the number of zero points of pressure between the boundary and the jet axis). The dashed lines show the modes of the  $u^+$  family. Only harmonics of mode  $m = 0$  are shown.  $\theta_j = 20^\circ$ ,  $M = 0.5$ ,  $kr = 5$ .

wave energy density  $E_0$  in the reference frame comoving with the medium (Landau & Lifshitz, 1987):

$$E = E_0 \frac{\omega}{\omega - \mathbf{kV}}. \quad (38)$$

Note that although formula (38) was initially derived for acoustic waves, it is of universal nature, because it allows simple quantum interpretation. Namely, the number of photons of the wave field  $\mathcal{N} = 2\pi E/h\omega = 2\pi E_0/h(\omega - \mathbf{kV})$  does not depend on the choice of the reference frame (Landau & Lifshitz, 1987).

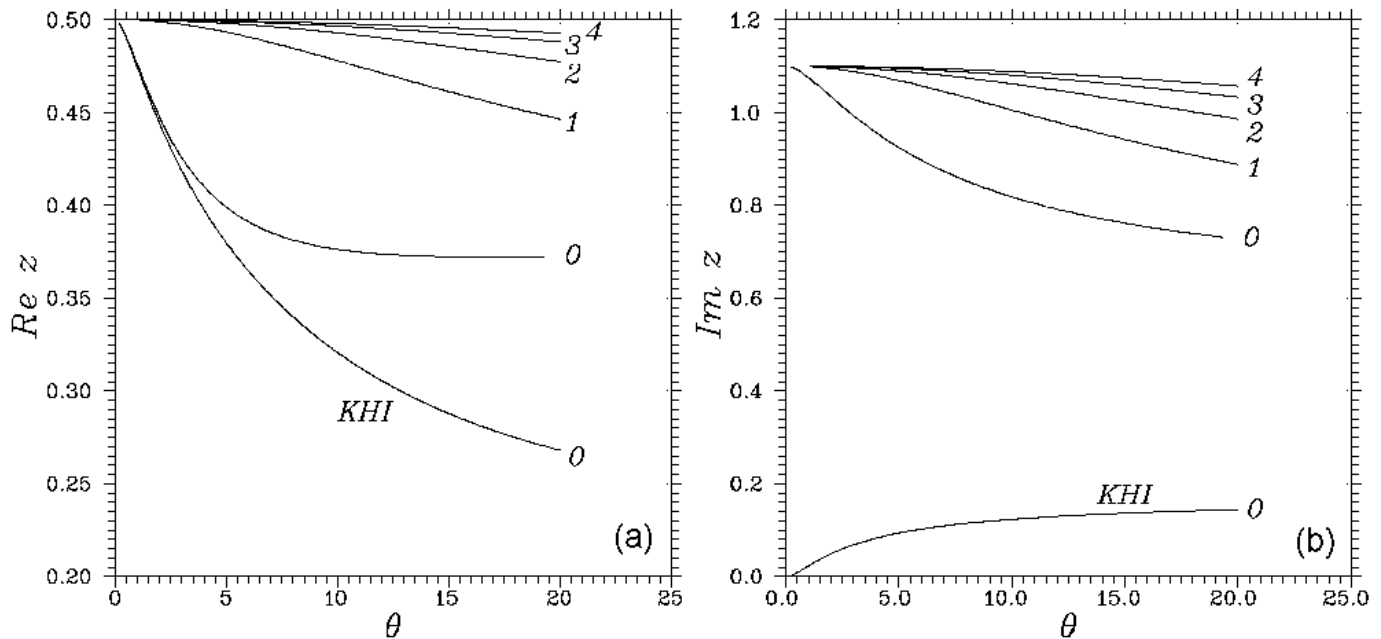


**Fig. 8.** Dependences of dimensionless phase velocities  $Re(\omega/kc_j)$  (a) and amplitude increments  $Im(\omega/kc_j)$  (b) on the jet half-opening angle  $\theta_j$  for different unstable modes. Each curve is labelled by the number of the harmonic (the number of pressure zero points between the boundary and axis of the jet). Only harmonics of mode  $m = 0$  are shown.  $kr = 5$ ,  $\tau = 5$ .

Thus modes of the  $u^+$  family, for which  $Re \omega > kV_j$  ( $Re z > M$ ), have positive energy density in the jet, whereas modes of the  $u^-$  family, for which  $0 < Re \omega < kV_j$  ( $0 < Re z < M$ ), have negative energy density. Therefore the decrease of the wave energy due to radiative cooling decreases the energy of  $u^+$ -family modes, and, correspondingly, results in their decay. And vice versa, the decrease of the wave energy due to radiative cooling increases the absolute value of the energy density of  $u^-$ -family modes and results in their amplification. The latter situation is a typical example of radiative and dissipative instability.

Like in the case of a medium without dissipation the dispersion law depends only very slightly on the change of the jet opening angle over a wide range of its values (Fig. 8).

Fig. 9 shows how the frequency of unstable perturbations depends on dimensionless wavenumber  $kr$ . It is convenient to normalize this frequency not to the frequency of acoustic waves, which itself depends on  $k$ , but to the characteristic frequency of IGWs — the Brunt-Väisälä frequency:

$$N^2 = \frac{1}{\rho_j} \frac{dP_j}{dr} \left( \frac{1}{\rho_j} \frac{d\rho_j}{dr} - \frac{1}{\rho_j c_j^2} \frac{dP_j}{dr} \right) = \frac{3\gamma - 1}{\gamma^2} \frac{c_j^2}{r^2}. \quad (39)$$

As is evident from Fig. 9b, our analysis predicts unlimited decrease of the characteristic time scale of the growth of unstable IGW modes with decreasing radial wavelength. One must nevertheless bear in mind that the presence of a transitional layer of finite thickness  $l$ , where velocity varies smoothly from  $V_j$  inside the jet to zero outside the jet, stabilizes perturbations with wavelength  $\lambda \leq l$ .

The characteristic feature of the IGW modes considered is that the maximum of perturbed pressure is achieved at the jet boundary, whereas both the perturbed displacement  $\xi$  of this boundary in the direction transversal to it and density perturbation are equal to zero in the adiabatic case and increase insignificantly with increasing parameter  $\tau$ . Moreover, outside the jet the perturbation amplitudes decrease very rapidly with the distance from the jet due to the difference of the impedances of the media:  $\rho_j c_j < \rho_a c_a$ . We show in Paper II that during the linear stage of the development of instability the initial flow (i.e., the jet proper) is not destroyed because of the smallness of the  $\theta$ -displacement, and perturbations remain localized inside a cone near the jet.

In conclusion, we make two small comments. First, although Figs. 6–9 show the dispersion curves only for axisymmetric pinch modes, the results for helical ( $m \geq 1$ ) modes are qualitatively the same. Second, the computations for bipolar outflows with the subsequent change of the boundary condition (30) yield the results that are identical to those that we discuss here for unipolar outflow. This conclusion follows directly from the localization of unstable modes near the jet boundary that we discuss in this paper.

## 5. Conclusions

Our linear analysis leads us to conclude that:

- Conical mass outflows in a field of quadratic gravitational potential and similar to those observed in a number of Seyfert galaxies are unstable against the

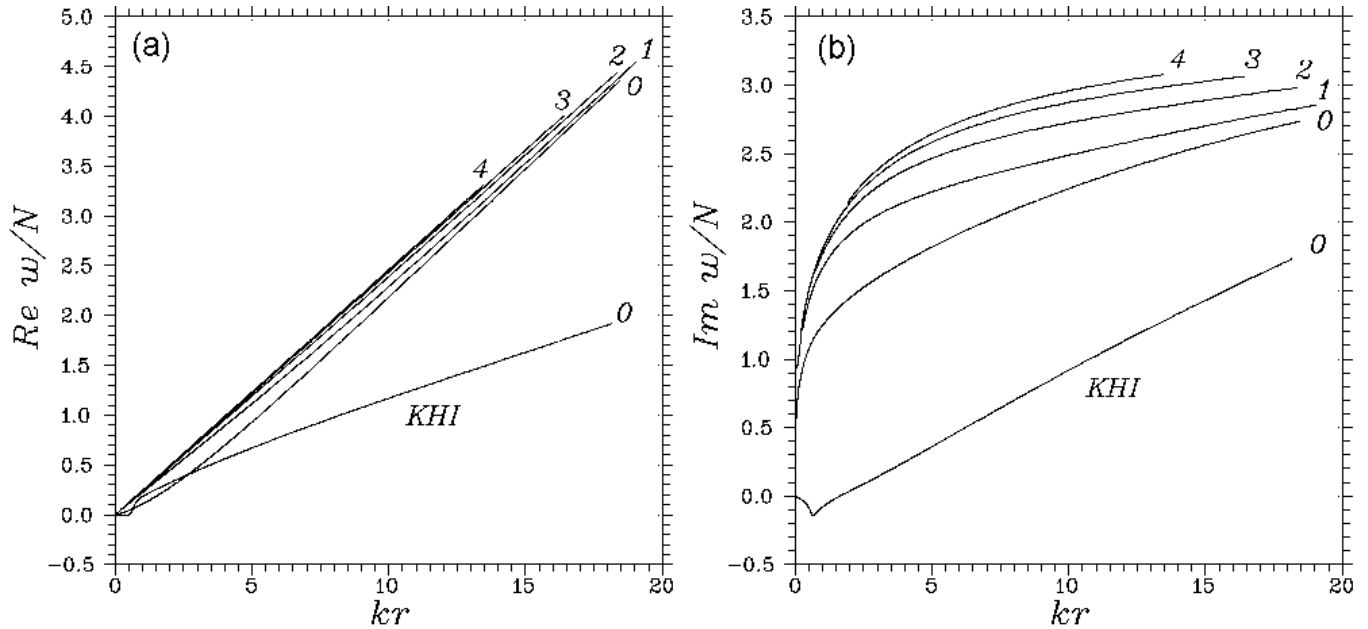


**Fig. 9.** Dependences of dimensionless frequency  $Re(\omega/N)$  (a) and increment  $Im(\omega/N)$  (b) on dimensionless radial wavenumber  $kr$  for different unstable modes. Each curve is labelled by the number of the harmonic (the number of zero points of pressure between the boundary and axis of the jet). Only the harmonics of mode  $m = 0$  are shown.  $M = 0.5$ ,  $\theta_j = 20^\circ$ ,  $\tau = 5$ .

resonance–waveguide development of a wide spectrum of pinch and helical internal gravity waves.

- The characteristic amplitude growth time scale of these modes depends extremely slightly on the jet opening angle over a wide range of these angles.
- Radiative cooling suppresses completely all gravitational acoustic waves, has only a slight effect on unstable surface Kelvin–Helmholtz modes, and results in the decay of waveguide–resonance internal gravity modes propagating in antisource direction relative to the jet matter. And vice versa, radiative cooling increases substantially the instability of such sourceward-propagating modes.
- amplification mentioned above has the form of radiative and dissipative instability of modes with negative energy density.
- the formation of the observed regular patterns in radiation cones in the vicinity of the nuclei of Seyfert galaxies can be due only to unstable surface modes and slow (sourceward moving in the jet) waveguide–resonance IGWs modes. The velocities of these modes along the jet boundary exceed the characteristic sound speed in the ambient atmosphere and this fact allows us to believe in their possible evolution into shocks.
- In the case of small jet opening angles the main harmonic of the pinch mode of IGWs is most likely to develop in the short-wavelength domain ( $kr \geq 20$ ). In the longer-wavelength domain ( $5 \leq kr \leq 15$ ) the main harmonic of the first helical mode is most likely to develop.
- Because of the different localization of the first helical and pinch modes the development of one of these

modes should not have fatal consequences whatsoever for the other mode.

We describe detailed numerical simulations of the development of these waves in our forthcoming Paper II.

## References

- Afanasiev V.L., Dodonov S.N., Khrapov S.S., Moiseev A.V., Mustsevoy V.V., 2007, *Astrophysical Bulletin* **62**, 17 (Paper I)
- Antonucci, R., 1993, *ARA&A*, **31**, 473
- Capetti A., Axon D.J., Macchetto F., Sparks W.B., Boksenberg A., 1996, *ApJ*, **469**, 554
- Capetti A., Axon D.J., Macchetto F., Marconi F.D., Winge C., 1999, *ApJ*, **516**, 187
- Emsellem E., Fathi K., Wozniak H., Ferruit P., Mundell C.G., Schinnerer E., 2006, *MNRAS*, **365**, 367
- Falcke H., Wilson A.S., Simpson C., Bower G.A., 1996, *ApJ*, **470**, L31
- Falcke H., Wilson A.S., Simpson C., 1998, *ApJ*, **502**, 199
- Ferrari A., Massaglia S., Trussoni E., 1982, *MNRAS*, **198**, 1065
- Ferruit P., Wilson A.S., Falcke H. et al. 1999, *MNRAS*, **309**, 1
- Hardee P.E., Norman M.L., 1988, *ApJ*, **334**, 70
- Kaiser M.E., Bradley L.D., Hutchings J.B., Crenshaw D.M. et al., 2000, *ApJ*, **528**, 260
- Landau L.D., Lifshitz E.M., 1987, book *Fluid Mechanics* 2nd ed. Pergamon Press, (Course of Theoretical Physics, v. 6)
- Levin K.A., Mustsevoi V.V., Khrapov S.S., *Astronom. Rep.*, 1999, **43**, 104
- MacDonald J., Bailey M.E., 1981, *MNRAS*, **197**, 995
- Miles J.W., 1957, *J. Acoust. Soc. Amer.*, **29**, 226
- Miyaji T., Wilson A.S., Perez-Fournon I., 1992, *ApJ*, **385**, 137
- Moiseev A.V., Afanasiev V.L., Dodonov, S.N., Khrapov, S.S., Mustsevoy, V.V., 2000, poster presented on JENAM-2000, astro-ph/0006323

- Morse J. A., Cecil G., Wilson A.S., Tsvetanov Z.I., 1998, ApJ, **505**, 159
- Mulchaey J.S., Tsvetanov Z., Wilson A.S., Perez-Fournon I., 1992, ApJ, **394**, 91
- Nagar N.N., Wilson A.S., Mulchaey J.S., Gallimore J.F., 1999, ApJS, **120**, 209
- Norman M.L., Hardee P.E., 1988, ApJ, **334**, 80
- Norman M.L., Stone J.M., 1997, ApJ, **483**, 121
- Payne D.G., Cohn H., 1985, ApJ, **291**, 655
- Pogge R.W., 1989, ApJ, **345**, 730
- Pogge R.W., De Robertis M.M., 1993, ApJ, **404**, 563
- Ribner H.S., 1957, J. Acoust. Soc. Amer., **29**, 435
- Rossi P., Capetti A., Bodo G. et al., 2000, A&A, **356**, 73
- Sofue Y., Rubin V., 2001, ARA&A, **39**, 137
- Steffen W., 1997, Vistas in Astronomy, **41**, 71 (astro-ph/9611133)
- Tsvetanov Z.I., Walsh J.R., 1992, ApJ, **386**, 485
- Veilleux S., Tully R.B., Bland-Hawtorn J., 1993, AJ, **105**, 1318
- Wills B.J., 1999, “Quasars and Cosmology” (ed by G. Ferland & J. Baldwin), ASP Conf.Series, **162**, 101 (astro-ph/990503)
- Wilson A.S., 1993, in “Astrophysical Jets”, STScl Symp. Series N 6, Cambridge Univ. Press, 121
- Wilson A.S., Tsvetanov Z.I., 1994, AJ, **107**, 1227

## Appendix A: Dispersion relation for IGWs

Here we briefly describe the derivation of the dispersion relation for internal gravity waves. We consider low-amplitude waves in a compressible medium with vertical density stratification due to uniform gravitational field  $-g\mathbf{e}_z$ , where  $g = \text{const}$ . The initial linearized set of hydrodynamics equations has the following form:

$$\frac{\partial \tilde{\rho}}{\partial t} + \tilde{v}_z \frac{\partial \rho_0}{\partial z} + \rho_0 \left( \text{div}_{\perp} \mathbf{v}_{\perp} + \frac{\partial \tilde{v}_z}{\partial z} \right) = 0, \quad (\text{A.1})$$

$$\frac{\partial \tilde{\mathbf{v}}_{\perp}}{\partial t} = -\frac{1}{\rho_0} \nabla_{\perp} \tilde{p}, \quad (\text{A.2})$$

$$\frac{\partial \tilde{v}_z}{\partial t} = -\frac{1}{\rho_0} \frac{\partial \tilde{p}}{\partial z} - g \frac{\tilde{\rho}}{\rho_0}, \quad (\text{A.3})$$

$$\frac{\partial \tilde{p}}{\partial t} + \tilde{v}_z \frac{\partial p_0}{\partial z} = c_s^2 \left( \frac{\partial \tilde{\rho}}{\partial t} + \tilde{v}_z \frac{\partial \rho_0}{\partial z} \right). \quad (\text{A.4})$$

Here subscript  $z$  denotes vertical components and subscript  $\perp$ , the vector components orthogonal to  $\mathbf{e}_z$ . The equation of hydrostatic equilibrium can be written in the following form:

$$g = -\frac{1}{\rho_0(z)} \frac{dp_0(z)}{dz}. \quad (\text{A.5})$$

Other designations are the same as in the main part of the paper.

We consider short-wavelength perturbations along the  $z$  axis:

$$\frac{1}{k_z} \left| \frac{\partial \ln \rho_0}{\partial z} \right| \ll 1, \quad (\text{A.6})$$

where  $k_z$  is the vertical component of wave vector  $\mathbf{k}$  ( $\mathbf{k}^2 = k_z^2 + \mathbf{k}_{\perp}^2$ ). We then seek a solution in the form of planar waves:

$$\tilde{f}(x, y, z, t) = \hat{f} \exp\{ik_x x + ik_y y + ik_z z - i\omega t\}, \quad (\text{A.7})$$

where  $\tilde{f}$  is the perturbed function with amplitude  $\hat{f} = \text{const}$ . The set of differential equations (A.1)–(A.4) transforms into the following algebraic equations:

$$-i\omega \hat{\rho} + \hat{v}_z \frac{d\rho_0}{dz} + i\rho_0(\mathbf{k}_{\perp} \hat{\mathbf{v}}_{\perp} + k_z \hat{v}_z) = 0, \quad (\text{A.8})$$

$$-i\omega \hat{\mathbf{v}}_{\perp} = -i\mathbf{k}_{\perp} \frac{\hat{p}}{\rho_0}, \quad (\text{A.9})$$

$$-i\omega \hat{v}_z = -ik_z \frac{\hat{p}}{\rho_0} - g \frac{\hat{\rho}}{\rho_0}, \quad (\text{A.10})$$

$$-i\omega \hat{p} - \rho_0 g \hat{v}_z = c_s^2 \left( -i\omega \hat{\rho} + \hat{v}_z \frac{d\rho_0}{dz} \right). \quad (\text{A.11})$$

This equation set is homogeneous and has a nontrivial solution only if its determinant is identically equal to zero. The latter condition yields the following dispersion equation:

$$\omega^4 + \omega^2 \left( -k_{\perp}^2 c_s^2 + g \frac{d \ln \rho_0}{dz} \right) - g k_{\perp}^2 \left( g + c_s^2 \frac{d \ln \rho_0}{dz} \right) = 0. \quad (\text{A.12})$$

In the case of a medium moving with velocity  $\mathbf{V}$  the Doppler transform for frequency  $\hat{\omega} = \omega - \mathbf{k}\mathbf{V}$  yields equation (35) in the main part of the paper.

*Acknowledgements.* We are grateful to I. G. Kovalenko for his critical comments and to V. V. Levi for numerous useful discussions. The images of the NGC 3516 and NGC 5252 galaxies were obtained with the 6-meter telescope of the Special Astrophysical Observatory of the Russian Academy of Sciences funded by the Ministry of Science of the Russian Federation (registration number 01-43). This work was supported in part by the “Nonstationary objects in the Universe” program of the Ministry of Industry and Science of the Russian Federation. A. V. Moiseev and V. L. Afanasiev also acknowledge the of from the Russian Foundation for Basic Research (project no. 06-02-16825).